Rapidly Solidified Lead Tin Calcium Alloys for Lead Acid Batteries

M. Kamal[1], R. M. Shalaby[1], T. El Ashram[2*], S. M. Abdelaty[2], A. Hany[2]

[1]Physics Department, Faculty of Science, Mansoura University, Mansoura, Egypt

[2]Physics Department, Faculty of Science, Port Said University, Port Said, Egypt

* Corresponding author: tnelashram@sci.psu.edu.eg.com

ABSTRACT

The effect of addition of Ca on the structure, thermal, mechanical, electrical and electrochemical properties of Pb-10Sn alloy was investigated for lead acid batteries applications in order to extend the life cycle of the gird by improving its mechanical and corrosion resistance. The material of lead acid battery grid mostly is based on Pb-Sn alloy. In the present work six rapidly solidified alloys of compositions (90-x)Pb-10Sn-xCa (x=0, 0.5, 1, 1.5, 2, 2.5 wt.%), were produced by melt-spinning technique. X-ray diffraction analysis and differential scanning calorimetry have been carried out. Also mechanical, electrical and electrochemical properties were measured. Here we show that the addition of 2.5 wt.% Ca to Pb-10Sn improves its mechanical properties this is evident in the increase of Young's modulus, microhardness number and microcreep behavior and enhances its corrosion resistance. Therefore the rapidly solidified melt-spun 87.5 wt.%Pb-10wt.%Sn-2.5wt.%Ca alloy is the most suitable alloy to be used as a grid in lead acid batteries.

Keywords

Melt spinning technique, mechanical properties, microcreep, electrical properties.

1. INTRODUCTION

Lead acid battery (LAB) is an electrical power source for many applications such as vehicles, submarines and emergency systems. LAB has many advantages like low cost, high voltage per cell and good capacity life [1] however it needs to extend deep cycle life. The improvement of the life time depends on the grid materials. The primary properties of interest in grid alloys for LAB are the mechanical strength and corrosion resistance, as well as the compatibility with the active materials and the electrochemical properties. Pb-Sn, Pb-Sb and Pb-Ca-Sn alloys are commonly used in the production of both valves regulated lead acid (VRLA) and starting lighting and ignition (SLI) batteries however Pb-Sb alloys corrode more rapidly than Pb-Sn [2,3]. Addition of 1wt.% Sn to Pb is better corrosion resistance than 1wt.% of Sb [4]. Pb-Ca, Pb-Sb and Pb-Ca-Sn alloys are commonly used in the production of positive and negative grids, connectors, posts and straps components of lead acid batteries [5-12].

Mustafa Kamal et al [13] reported that the composition of alloys plays an important role on grid battery performed and it is observed that Pb-0.5Sn-0.1Ca alloy can be used as grids for lead acid batteries. The addition of tin up to 1.2 wt.% and addition of silver up to 0.05 wt.% increase the mechanical properties and corrosion resistance of Pb-0.08Ca–0.013 Al alloy. Also the addition of aluminum was studied and it was found that aluminum prevents calcium oxidation [14-16]. According to the previous studies shown above the aim of the present work is to study the effect of addition of Ca and rapid solidification using melt spinning technique on the structure, physical and electrochemical properties of Pb-Sn alloys to be used as grids for lead acid batteries.

2. EXPERIMENTAL PROCEDURES

Six alloys of compositions (90-x)Pb-10Sn-xCa (x= 0, 0.5, 1, 1.5, 2, 2.5 wt.%) were produced by a single copper roller melt-spinning technique. The quantities of these metals were weighted out and melted in a porcelain crucible. The casting was done in air at melting temperature of 700 °C. The speed of the copper wheel was fixed at 2900 rpm, which corresponds to a linear speed of 30.4 ms^{-1}. X-ray diffraction (XRD) analysis was carried out with a Shimadzu X-ray diffractometer DX-30, using Cu Kα radiation with Ni filter (λ = 0.154056 nm). Differential scanning calorimetry (DSC) was carried out with heating rate 10 K/min and the system was calibrated using a standard sample. The electrical resistivity was measured by the double bridge method. A digital Vickers microhardness tester model-FM-7 was used to measure Vickers microhardness number HV and microcreep as developed and confirmed by T. El Ashram [17-18]. In this method the fractional increase in the area of indentation is considered to be the strain. It was found that this strain increases by increasing the indentation time from which microcreep behavior can be determined. The potentiodynamic current-potential curves were recorded by changing the electrode potential automatically from -500 to 500 mV in case of C-steel with scanning rate 5 mVs^{-1} by using computer controlled potentiostate Gamry PCI4-G750 with DC 105 software for calculations and storted the data.

3. RESULTS AND DISCUSSION

3.1 Crystal Structure

Fig. 1 shows the XRD patterns for as-quenched melt-spun ribbons of compositions (90-x)Pb-10Sn-xCa (x= 0, 0.5, 1, 1.5, 2, 2.5 wt.%). Fig. 1a, for Pb-10Sn alloy, shows that the eutectic mixture of Pb and Sn phases. The same structure was found for Pb-10Sn-0.5Ca, Pb-10Sn-1Ca and Pb-10Sn-1.5Ca alloys as shown in Fig. 1b, Fig. 1c and Fig. 1d respectively. There is no precipitation of Ca observed in these alloys all Ca atoms were dissolved in the matrix. In Fig. 1e, for Pb-10Sn-2Ca, formation of $CaPb_3$ intermetallic compound was observed at 2θ = 31.79°, 41.57°, 56.25°, 59.73° and 67.89°. Formation of $CaPb_3$ intermetallic compound was also observed for Pb-10Sn-2.5Ca (Fig. 1f) at 2θ =40.89°, 56.13°, 83.41° and 86.56°.The matrix is a solid solution of Sn in Pb with cubic crystal system and space group Fm$\overline{3}$m. Sn phase has tetragonal crystal system and space group I4$_1$/amd. $CaPb_3$ intermetallic compound has cubic crystal system with space group Pm$\overline{3}$m. It has a primitive cubic lattice with one molecule per lattice point. The lattice parameter *a* of Pb matrix was calculated from the peak position of highest intensity which corresponding to the plane (111). The variation of lattice parameters and volume of the unit cell of matrix is shown in Table 1. The lattice parameter *a* was increased by the addition of Ca from 4.9483 Å for Pb-10Sn to 4.9857 Å for Pb-10Sn-1.5Ca alloy and then decreased to 4.9608 Å for Pb-10Sn-2Ca alloy.
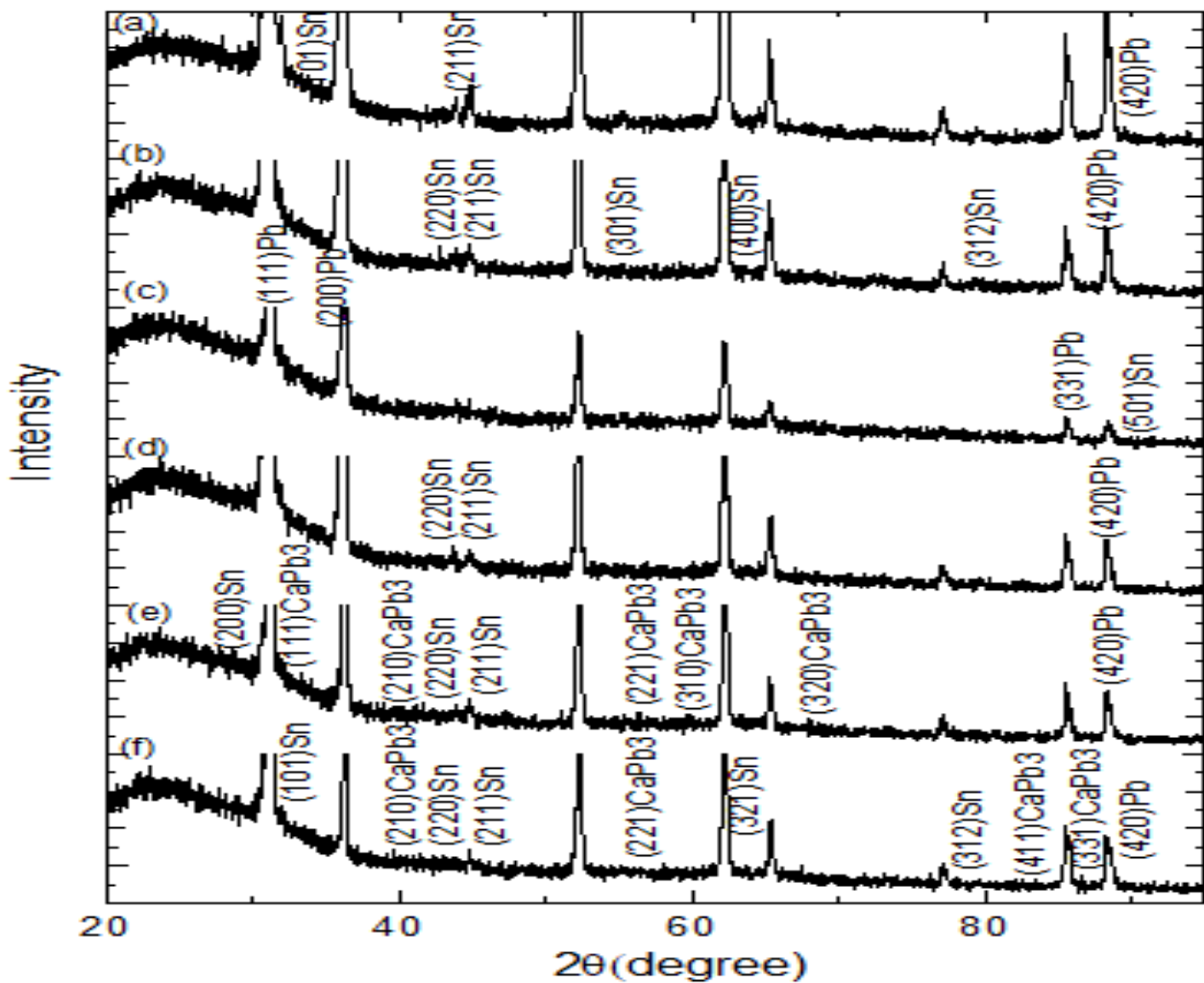
Fig.1 XRD patterns of (90-x)Pb-10Sn-xCa (x= 0, 0.5, 1, 1.5, 2, 2.5 wt. %) alloys

The increase in a may be due to the dissolving of Ca atom, which has large radius compared to Pb and Sn atoms, in Pb lattice. The decrease in a, which was observed for Pb-10Sn-2Ca alloy, may be due to the formation of $CaPb_3$ intermetallic compound in that alloy. The same behavior was observed for the volume of unit cell v of the matrix since $v = a^3$.

Table 1 Details of XRD analysis of (90-x)Pb-10Sn-xCa (x= 0, 0.5, 1, 1.5, 2, 2.5 wt. %) alloys

Alloys	Phases present	Lattice parameter of the matrix a (Å)	Unit cell volume v (Å)^3
Pb-10Sn	Pb, Sn	4.9483	121.17
Pb-10Sn-0.5Ca	Pb, Sn	4.9466	121.04
Pb-10Sn-1Ca	Pb, Sn	4.9474	121.10
Pb-10Sn-1.5Ca	Pb, Sn	4.9857	123.93
Pb-10Sn-2Ca	Pb, Sn, $CaPb_3$	4.9608	122.08
Pb-10Sn-2.5Ca	Pb, Sn, $CaPb_3$	4.9459	120.99

3.2 Thermal Analysis

The DSC curves for Pb-10Sn, Pb-10Sn-1.5Ca and Pb-10Sn-2.5Ca melt- spun alloys are shown in Fig. 2. It shows that the transition to the α -Pb phase occurred at about 181.3 °C for Pb-10Sn (Fig. 2a) alloy rapidly solidified while this transition occurs at about 150 °C for conventional Pb-10Sn according to the equilibrium phase diagram. This variation may be attributed the high concentration of point defects introduced by rapid solidification. These defects need more heat to be recovered before the transition to the ordered α-Pb phase. The same behavior was observed for Pb-10Sn-1.5Ca (Fig. 2b) and Pb-10Sn-2.5 Ca (Fig. 2c). The solidus T_s, liquidus T_l and melting temperatures T_m were determined. Also the enthalpy of fusion ΔH and the pasty range were determined from the DSC curves as shown in Table 2. A slight increase in the melting temperature from 297.43°C for Pb-10Sn to 298.13 °C for Pb-10Sn-2.5Ca occurred due to the addition of Ca. Also a slight increase in the ΔH from 28.91 Jg^{-1} for Pb-10Sn to 29.12 Jg^{-1} for Pb-10Sn-2.5Ca occurred due to the addition of Ca. The pasty range was also increased from 17.89 °C for Pb-10Sn to 20.33 °C for Pb-10Sn-2.5Ca. The slight increase in the thermodynamic parameters may be attributed to the formation of CaPb$_3$ intermetallic compound.
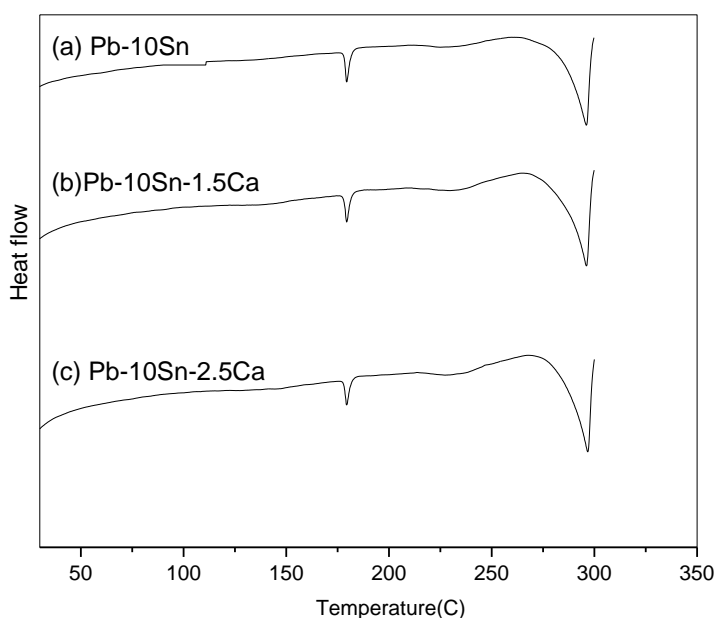
Fig. 2 Differential scanning calorimetry (DSC) curves for melt spun Pb-10Sn-xCa (x= 0, 1.5, 2.5 wt.%) alloys

Table 2 Details of DSC analysis of Pb-10Sn-xCa (x= 0, 1.5, 2.5 wt. %) alloys.

Alloy	T_s (°C)	T_l (°C)	Pasty Range (°C)	T_m (°C)	ΔH (J g^{-1})
Pb-10Sn	286.1	303.99	17.89	297.43	28.91
Pb-10Sn-1.5Ca	286.09	305.08	15.99	297.5	31.58
Pb-10Sn-2.5Ca	285.41	305.74	20.33	298.13	29.12

3.3 Mechanical Properties

3.3.1 Young's Modulus And Internal Friction

Fig. 3a shows the variation of Young's modulus (E) with the variation of Ca concentration of as-quenched melt-spun Pb-10Sn-xCa (x =0, 0.5, 1, 1.5, 2, 2.5 wt.%) alloys. The value of E for Pb-10Sn was found to be 24.49 GPa. The addition of Ca decreases E to minimum value about 16.6 GPa and then increases gradually to maximum value 39.93 GPa for Pb-10Sn-2.5Ca alloy. The decrease in E may be due to dissolving Ca atoms in the Pb lattice cause attenuation to the bond strength between Pb atoms and hence decrease E. The increase in E can be attributed to the formation of $CaPb_3$ intermetallic compound which is hard phase dispersed in the Pb matrix. Fig. 3b. shows the variation of internal friction (Q^{-1}) with the variation of Ca concentration. It shows that (on the average) Q^{-1} decreases with increasing Ca addition from 0.112 for Pb-10Sn alloy to minimum value 0.018 for Pb-10Sn-2.5Ca alloy. The decrease in Q^{-1} may be due to Ca atoms that dissolved in Pb lattice prevent the motion of substitutional Sn atoms in the Pb lattice.
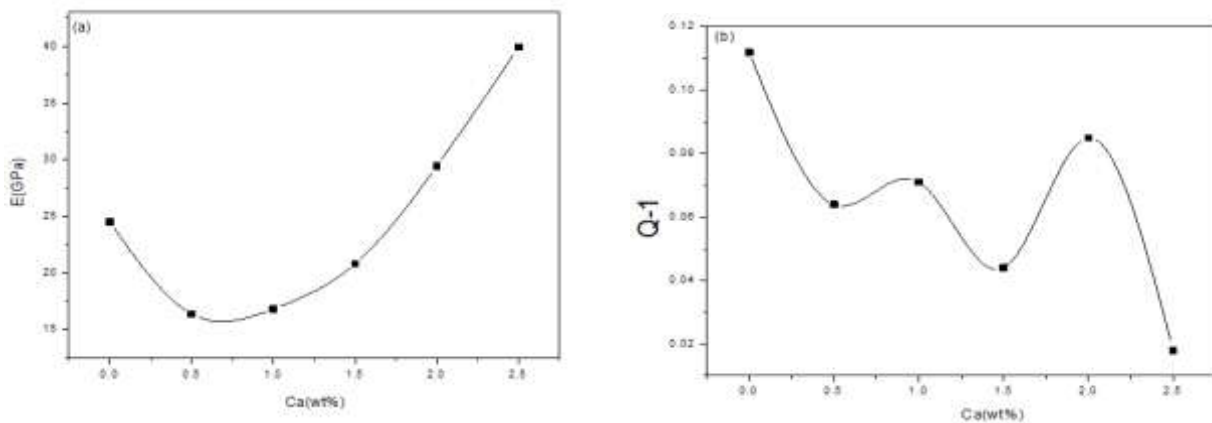
Fig. 3 Variation of (a) Young's Modulus and (b) internal friction with Ca concentration for melt-spun Pb-10Sn-xCa (x= 0, 0.5, 1, 1.5, 2, 2.5 wt.%) alloys

3.3.2 Microhardness

Fig. 4 shows the variation of HV with Ca concentration of as-quenched melt -spun Pb-10Sn-xCa (x=0, 0.5, 1, 1.5, 2, 2.5 wt.%) alloys. HV was found to be 113.6 MPa for Pb-10Sn alloy and then decreased by addition of Ca to 95.55 MPa for 0.5 wt.% Ca. HV was gradually increased to 95 134.26 MPa for 2 wt.%Ca and 137.69 MPa for 2.5 wt.%Ca. The decrease of HV may be due to the presence of Ca atoms in the Pb lattice and this causes local elastic strain which facilities the motion of dislocations. The increase of HV may be due to the dispersion hardening of $CaPb_3$ intermetallic compound that dispersed in the Pb matrix.

3.3.3 Microcreep

Fig. 5a shows the variation of HV with indentation time, in time interval from 5 to 99 s. It is obvious that HV for all alloys decreases by increasing dwell time. Using the method developed by T. El Ashram [17] we can determine the microcreep behavior. Fig. 5b shows the microcreep behavior of as-quenched melt-spun Pb-10Sn-xCa (x=0, 0.5, 1, 1.5, 2, 2.5 wt.%) alloys by plotting the strain with indentation time in time interval from 5 to 99 s. All alloys (except 2 and 2.5 wt.% Ca that contain $CaPb_3$ intermetallic compound) exhibit the three stages of creep, while, the other two alloys exhibit only the secondary stage. This indicates the high creep resistance of these alloys due to the dispersion of $CaPb_3$ intermetallic particles.
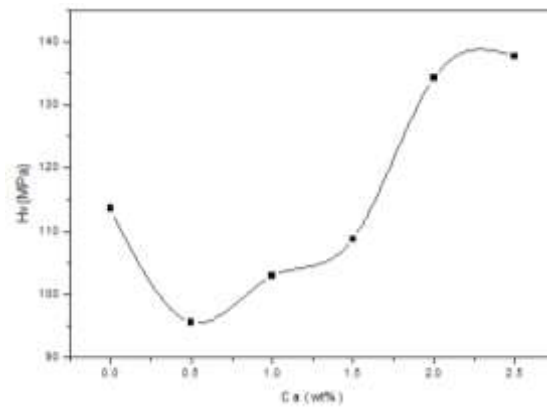
Fig 4 The variation of HV with Ca concentration for as-quenched melt-spun Pb-10Sn-xCa

(x=0, 0.5, 1, 1.5, 2, 2.5 wt.%) alloys
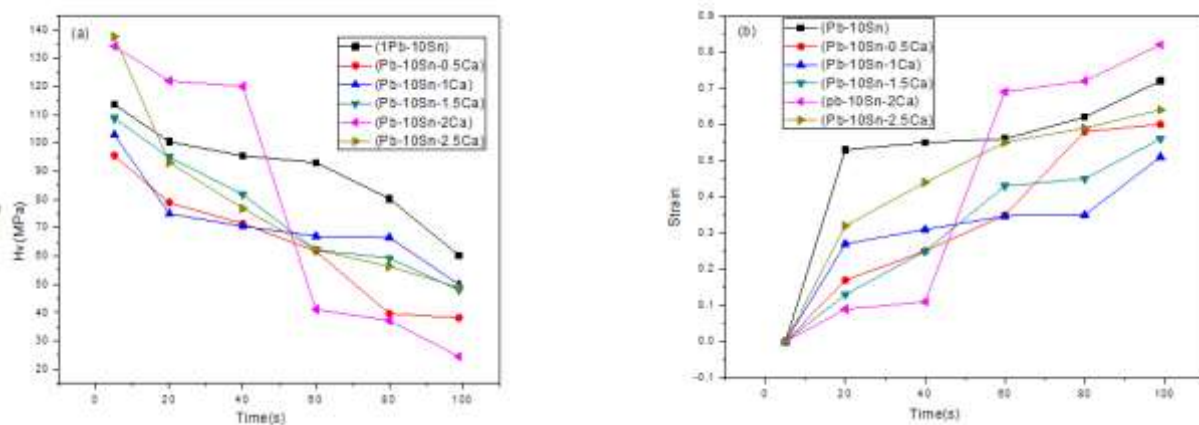
Fig. 5 The variation of (a)Vickers microhardness number (HV) and (b) Microcreep behavior in which the strain is plotted versus dwell time for as-quenched melt-spun Pb-10Sn-xCa (x=0, 0.5, 1, 1.5, 2, 2.5 wt.%)

3.3.4 Electrical Resistivity

The measured electrical resistivity of as-quenched melt -spun Pb-10Sn-xCa (x=0, 0.5, 1, 1.5, 2, 2.5 wt.%) alloys at room temperature is shown in Table 3. The addition of 0.5 wt.% Ca increases the resistivity from 15.95 to 22.7 x10^{-8} Ω.m. This may be due to the scattering of conduction electrons with Ca solute atoms. For 1wt.% Ca and 1.5 wt.% Ca additions the resistivity decreases to 15.23 and 14.75x$10^{-8}\Omega$.m respectively. This can be explained in terms of the reduction of Pb ratio due to the addition of Ca, and the resistivity of Pb is six times that of Ca. Finally for 2wt.% Ca and 2.5 wt.% Ca additions the resistivity increases to 32.83 and 29.25x10-8 Ω.m respectively. This can be attributed to the formation of CaPb$_3$ intermetallic particles that dispersed in the Pb matrix.

Table 3 Electrical resistivity of as-quenched melt –spun (90-x)Pb-10Sn-xCa (x=0, 0.5, 1, 1.5, 2, 2.5 wt.%) alloys

Alloy	Electrical Resistivity at RT $\rho x 10^{-8} \Omega.m$
Pb-10Sn	15.95
Pb-10Sn-0.5Ca	22.70
Pb-10Sn-1Ca	15.23
Pb-10Sn-1.5Ca	14.75
Pb-10Sn-2Ca	32.83
Pb-10Sn-2.5Ca	29.25

3.3.5 Electrochemical Properties

Potentiodynamic polarization curves for Pb-10Sn-xCa (x=0, 0.5, 1, 1.5, 2, 2.5 wt.%) alloys in 0.1 N H_2SO_4 are shown in Fig. 6. From these curves the corrosion potential E_{Corr} and corrosion current I_{Corr} were determined. Then the corrosion rate was calculated for all alloys as shown in Table 4.
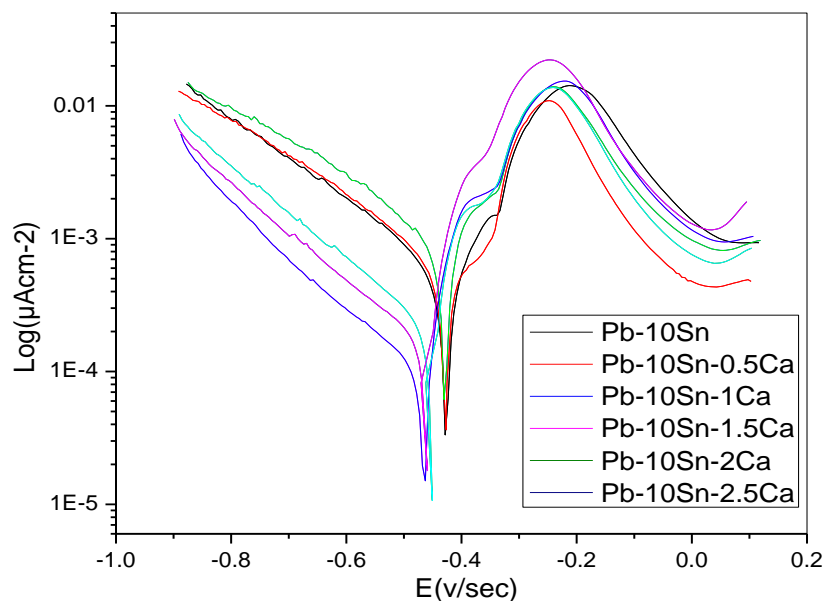
Fig. 6 Potentiodynamic polarization curves for Pb-10Sn-xCa (x=0, 0.5, 1, 1.5, 2, 2.5 wt.%) alloys in 0.1 N H_2SO_4

It is evident that the corrosion rate decreases by increasing Ca concentration to minimum value about 95.98 mpy for 2.5 Ca alloy. There are many factors affect corrosion such as the chemical composition and concentrations of the material under investigation and its environment, temperature, the crystal structure and microstructure of the material. All these factors were kept constant except the variation of Ca concentration.

Therefore Ca atoms may act as corrosion inhibitors in Pb-Sn alloy. This means that the addition of Ca atoms to enhances the corrosion resistance of Pb-10Sn alloys.

Table 4 corrosion potential E_{Corr}, corrosion current I_{Corr} and corrosion rate of Pb-10Sn-xCa (x=0, 0.5, 1, 1.5, 2, 2.5 wt.%) alloys in 0.1 N H_2SO_4

Alloy	I_{Corr} ($\mu A\ cm^{-2}$)	$-E_{Corr}$ (mV)	C. R (mpy)
Pb-10Sn	719	426	308.7
Pb-10%Sn-0.5%Ca	657	429	282.3
Pb-10%Sn-1%Ca	550	428	223.6
Pb-10%Sn-1.5%Ca	239	466	102.6
Pb-10%Sn-2%Ca	370	452	158.9
Pb-10%Sn-2.5%Ca	224	462	95.98

5. CONCLUSION

From the experimental results of structural analysis, physical and electrochemical measurements of rapidly solidified melt-spun Pb-10Sn-xCa (x=0, 0.5, 1, 1.5, 2, 2.5 wt.%) alloys, the following conclusion is obtained; The addition of 2.5 wt.% Ca to Pb-10Sn alloy improves its mechanical properties this is evident in the increase of Young's modulus and microcreep behavior and enhances its corrosion resistance. Therefore the rapidly solidified melt-spun 87.5Pb-10Sn-2.5Ca alloy is the most suitable alloy to be used as a grid in lead acid batteries

REFERENCES

[1]   Rand D. A. J., Moseley P. T., Garche J., and Parker C. D., Valve-Regulated Lead-Acid Batteries, Elsevier, Amsterdam, Netherlands, (2004).

[2]   Prengman R. D., J. Power Sources. 158 (2006) 1110.

[3]   REZAEI B., S. DAMIRI. Effect of solidification temperature of lead alloy grids on the electrochemical behavior of lead-acid battery. J. Solid State Electrochem. 9, 590–594, (2005).

[4]   BAKOUR Z. AND A. DAKHOUCHE, Electrochemical corrosion of Pb-Sn and Pb-Sb alloys for lead acid battery applications, International Advances in Applied Physics and Materials Science. 134 (2018) 103-105.

[5]   PEIXOTO L. C., W. R. OS´ORIO, AND A. GARCIA, The interrelation between mechanical properties, corrosion resistance and microstructureofPb-Sncastingalloysforlead-acidbatterycomponents. Journal of Power Sources. 195 (2010) 621–630.

[6]   SLAVKOV D., B.S. HARAN, B.N. POPOV, AND F. FLEMING, "Effect of Sn and Ca doping on the corrosion of Pb anodes in lead acid batteries," Journal of Power Sources. 112 (2002) 199– 208.

[7]   SIMON A. C. AND E. L. JONES, J ELECTROCHEM. SOC. 100(1953) IBID. 101(1954) 536.

[8]   BAKOUR Z. AND DAKHOUCHE A., Electrochemical corrosion of Pb-Sn and Pb-Sb alloys for lead acid battery applications, International Advances in Applied Physics and Materials Science. 134 (2018) 103-105.

[9]   ABU BAKR EL- BEDIWI, SANAA RAZZAQ ABBAS, RIZK MOSTAFA SHALABY, MUSTAFA KAMAL, "Study the Electrochemical Corrosion Behavior, Microstructure and Some

Physical Properties of Lead- Calcium Rapidly Solidified Alloys", Themed Section: Engineering and Technology. 1 (2015) 196-202.

[10]   DAVID R. PRENGMAN, "Challenges from corrosion-resistant grid alloys in lead acid battery manufacturing", Journal of power sources. 95 (2001) 224-233.

[11]   LAKSHMI C.S., MANDERSB AJ. E. . D. M. RICEB. "Structure and properties of lead–calcium–tin alloys for battery grids", Journal of power sources. 73 (1998) 23-29.

[12]   EJULLIAN L ALBERT J L CAILLERIE, "New lead alloys for high-performance lead–acid batteries", Journal of power sources. 116 (2003) 185-192.

[13]   MUSTAFA KAMAL, ABU-BAKR EL-BEDIWI, MOHAMMED.S. JOMAAN, "Rapid quenching of liquid lead base alloys for high performance storage battery applications", International Journal of Engineering & Technology IJET-IJENS. 12 (2015) 60-67.

[14]   ALBERTA. A. CHABROLB. L. TORCHEUXBPH. STEYERC. J.P. HILGERC. Improved lead alloys for lead/acid positive grids in electric-vehicle applications, Journal of power sources. 67 (1997) 257-265.

[15]   PANELY J-L CAILLERIE L. ALBERT, Lead calcium alloy development. Journal of power sources. 67 (1997) 279-281.

[16]   ZHONG S., WANG J., H. K. LIU, S. X. DOU, M. SKYLLAS-KAZACOS, Influence of silver on electrochemical and corrosion behaviors of Pb-Ca-Sn-Al grid alloys, Journal Of Applied Electrochemistry. 29 (1999) 177-183.

[17]   EL-ASHRAM T., R.M. SHALABY, "Effect of rapid solidification and small additions of Zn and Bi on the structure and properties of Sn-Cu eutectic alloy". J. Electron. Mater. 34 (2005) 212–215.

[18]   MUSTAFA KAMAL, TAREK EL ASHRAM, " Microcreep of rapidly solidified Sn-0.7wt.%Cu-In solder alloys", Materials Science and Engineering A 456 (2007) 1–4.